

Semi analytic approach to understanding the distribution of neutral hydrogen in the universe

T. Roy Choudhury[★], T. Padmanabhan[†], R. Srianand[‡]

IUCAA, Post Bag 4, Ganeshkhind, Pune 411 007, India.

Accepted 2000 December 00. Received 2000 December 00; in original form 2000 December 00

ABSTRACT

Analytic derivations of the correlation function and the column density distribution for neutral hydrogen in the intergalactic medium (IGM) are presented, assuming that the non-linear baryonic mass density distribution in the IGM is lognormal. We have compared the analytic results with observations and explored the possibility of constraining various cosmological and IGM parameters. Two kinds of correlation functions are defined : (i) along the line-of-sight (LOS) and (ii) across the transverse direction. Comparison of the observed LOS correlation with our analytical models suggests that unique recovery of power spectrum is difficult without a prior knowledge of the IGM parameters. However, we show that it is possible to constrain the slope of the equation of state of the IGM, γ , and its evolution using the observed LOS correlation function at different epochs. From the transverse correlation function, we obtain the excess probability, over random, of finding two neutral hydrogen overdense separated by an angle θ . We find that this excess probability is always less than 1% for redshifts greater than 2. Our models also reproduce the observed column density distribution for neutral hydrogen. We show that the shape of the distribution depends on γ . Our calculations suggest that one can rule out $\gamma > 1.6$ for $z > 2.31$ using the column density distribution. We suggest that the constraints on the evolution of γ (obtained using both the LOS correlation and the column density distribution) can be used as an independent tool to probe the reionisation history of the universe.

Key words: cosmology: large-scale structure of universe, power spectrum – intergalactic medium – quasars: absorption lines

1 INTRODUCTION

The nature and evolution of the initial power spectrum of density fluctuations could be obtained by studying the distribution of objects at different scales and different epochs. The formalism for studying the formation of structures with dark matter (DM) is well established, as they are collisionless particles interacting only through gravity, and is been extensively studied using the large cosmological N-body simulations. However, in order to model the evolution of baryonic structures like galaxies, groups of galaxies etc. one needs to incorporate all the hydrodynamical processes, ionisation, cooling, star formation etc., in the N-body simulations. Because of such complications, our understanding of the formation of baryonic structures has been limited.

Among the various baryonic structures, the regions where one can neglect the star formation, are comparatively easier to study. Two such areas are (a) low amplitude fluctuations in the intergalactic medium (IGM), where the star formation rate is very low, and (b) the intracluster medium, where one studies over large scales and thus the star formation details can be neglected. Hence considerable effort has been given in understanding these two types of structures.

The baryonic matter distribution at $z \leq 5$ is well probed through the absorption signatures they produce on the spectra of the distant QSOs. It is widely believed that while the metal lines systems (detected through Mg II or C IV doublets) seen in the QSO spectra could be associated with the halos of the intervening luminous galaxies (Bergeron & Boisse 1991; Steidel 1993), most of the low neutral hydrogen column density absorption lines (commonly called as ‘Ly α ’ clouds) are believed to be due to low amplitude fluctuations in the IGM.

Semi analytical as well as hydrodynamical simulations

[★] E-mail: tirth@iucaa.ernet.in

[†] E-mail: paddy@iucaa.ernet.in

[‡] E-mail: anand@iucaa.ernet.in

are consistent with the view that the Ly α clouds are small scale density fluctuations (Bond et al. 1988; Cen et al. 1994; Zhang, Anninos & Norman 1995; Hernquist et al. 1996; Miralda-Escudé et al. 1996; Bi & Davidsen 1997; Riediger et al. 1998; Theuns, Leonard & Efstathiou 1998; Theuns et al. 1998; Davé et al. 1999) that are naturally expected in any standard structure formation models. This idea is supported by the detection and the evolution of the weak clustering among the Ly α clouds in the redshift space (Cristiani et al. 1995; Srianand 1997; Khare et al. 1997). Subsequently it is realised that the thermal history of the Ly α line forming regions depends on (i) epoch of reionisation (equation of state) (ii) rate of photoionisation and (iii) adiabatic cooling. One can in principle neglect shocks and other processes that are important only in the highly non-linear regime. However a simple linear evolution of the densities will fail to produce the saturated Ly α systems and one needs to incorporate non-linearities in the model.

As a first step, one can model the non-linear evolution of the baryonic fluctuations that produce Ly α clouds using one of the several approximate models like: (i) Zeldovich approximation (Doroshkevich & Shandarin 1977; McGill 1990; Hui, Gnedin & Zhang 1997), (ii) lognormal approximation (Bi 1993; Gnedin & Hui 1996; Bi & Davidsen 1997), or (iii) power law approximation (Bi et al. 1995) (strictly speaking, the baryonic fluctuations are calculated here using the linear theory). In all these cases the baryon density is estimated from the DM density by some rule and the neutral fraction is estimated by considering the equilibrium between the rate of photoionisation due to background radiation and the rate of recombination estimated from the temperature defined through the equation of state. All these models depend on various IGM parameters such as intensity of the background radiation, equation of state and density average temperature as well as the cosmological parameters like Ω_m , Ω_Λ , etc.

Observationally the statistical properties of the Ly α absorption lines are quantified through the column density distribution, correlation functions and their dependence on the mean redshift. The clustering properties of the Ly α absorption lines are studied through two point correlation function obtained either (a) in the redshift space using the lines detected along a single line-of-sight (LOS) which we call ‘‘LOS correlation function’’, or (b) among the absorption lines detected along the lines of sights toward a few closely spaced QSOs which we call ‘‘transverse correlation function’’. In either case the observed spectra is decomposed into clouds using ‘‘Voigt’’ profile fits. Though this process smoothes the density field over the width of the lines the average effects due to thermal broadening is taken care of by the Voigt profiles. One can also compute the two-point correlation function of the observed flux in different pixels. Though this process does not decompose the actual density fields into cloudlets, in order to analyse the data the models should incorporate the thermal broadening and blending of contribution from different density fluctuations (Croft et al. 1999; McDonald et al. 1999). Most of the existing studies concentrate on obtaining constraints on the cosmological parameters using the observed statistical properties. Comparatively very less effort is directed to understand how the observed quantities depend on the IGM parameters.

In this work we make a preliminary attempt to investigate the dependence of the observable quantities on various

parameters of the models using a simple analytic approach. We derive analytic relations for the two-point correlation function among the Ly α clouds and the column density distribution using a lognormal approximation. These equations are used with the observed Voigt profile fitted data to get constraints on different IGM and cosmological parameters. In section 2, we treat the non-linear evolution with a simple ansatz proposed by Bi & Davidsen (1997) for the baryonic density fluctuations, and derive analytic expressions for the correlation function along the LOS and in the transverse direction and the column density distribution. In section 3, we study the correlation function at different redshifts for different structure formation models and for different values of the IGM parameters such as mean temperature and the equation of state. We compare our results with the existing observational data of Cristiani et al. (1997). We also present the results for the column density distribution and study its dependence on various cosmological and IGM parameters. The results are summarised in section 4.

2 ANALYTIC MODEL

The linear density contrast for dark matter in comoving k -space, for a particular redshift z , is given by

$$\delta_{\text{DM}}(\mathbf{k}, z) = D(z)\delta_{\text{DM}}(\mathbf{k}, 0), \quad (1)$$

where $D(z)$ is the linear growth factor for the density contrast, normalised such that $D(0) = 1$. If we assume the linear density contrast to be a Gaussian random field, then the corresponding linearly extrapolated power spectrum $P_{\text{DM}}(k)$ is defined by

$$\langle \delta_{\text{DM}}(\mathbf{k}, 0)\delta_{\text{DM}}(\mathbf{k}', 0) \rangle = (2\pi)^3 P_{\text{DM}}(k)\delta_{\text{Dirac}}(\mathbf{k} - \mathbf{k}'). \quad (2)$$

The power spectrum is only a function of the magnitude of \mathbf{k} , because of the isotropy of the background universe.

The linear density contrast for baryons in the IGM can be obtained from the DM density contrast by smoothing over scales below the Jeans length. We use the relation (Fang et al. 1993)

$$\delta_{\text{B}}(\mathbf{k}, z) = \frac{\delta_{\text{DM}}(\mathbf{k}, z)}{1 + x_b^2(z)k^2}, \quad (3)$$

where

$$x_b(z) = \frac{1}{H_0} \left[\frac{2\gamma k_B T_m(z)}{3\mu m_p \Omega_m(1+z)} \right]^{1/2} \quad (4)$$

is the Jeans length; T_m and μ are the density-averaged temperature and mean molecular weight of the IGM respectively; Ω_m is the cosmological density parameter of total mass and γ is the ratio of specific heats. Strictly speaking, equation (3) is valid only for the case $\gamma = 4/3$, but it is shown by Bi, Borner & Chu (1992) that equation (3) is a good approximation for $\delta_{\text{B}}(\mathbf{k}, z)$ even for $\gamma \neq 4/3$. The linear density contrast in real comoving space, $\delta(\mathbf{x}, z)$, is the Fourier transform of equation (3).

In principle, to study the properties of the IGM one has to take into account the non-linearities in the density distribution and various physical processes such as shocks, radiation field, cooling etc. However, detailed hydrodynamical modelling of IGM has shown that most of the low column density Ly α absorption (i.e. $N_{\text{HI}} \leq 10^{14} \text{ cm}^{-2}$) are

produced by regions that are either in the linear or in the weakly non-linear regime (Cen et al. 1994; Zhang, Anninos & Norman 1995; Hernquist et al. 1996; Miralda-Escudé et al. 1996; Theuns, Leonard & Efstathiou 1998; Theuns et al. 1998; Davé et al. 1999). The lower envelope of the column density, N_{HI} versus the thermal velocity dispersion, b (given by $b = (2k_B T/m_p)^{1/2}$) scatter plot (Schaye et al. 1999a; Schaye et al. 1999b) suggests that there is a well defined relationship between the density and the temperature of the IGM (Hui & Gnedin 1997). Thus it is possible to model low column density systems using simple prescription for the non-linear density field and an equation of state.

In this work, we take into account the effect of non-linearity by assuming the number density distribution of the baryons, $n_B(\mathbf{x}, z)$ to be a lognormal random field

$$n_B(\mathbf{x}, z) = A e^{\delta_B(\mathbf{x}, z)} \quad (5)$$

where A is a constant to be determined. The mean value of $n_B(\mathbf{x}, z)$ is given by

$$\langle n_B(\mathbf{x}, z) \rangle \equiv n_0(z) = A \langle e^{\delta_B(\mathbf{x}, z)} \rangle \quad (6)$$

Since $\delta_B(\mathbf{x}, z)$ is a Gaussian random field, one can write

$$\langle e^{\delta_B(\mathbf{x}, z)} \rangle = e^{\Delta^2(z)/2} \quad (7)$$

where

$$\Delta^2(z) = \langle \delta_B^2(\mathbf{x}, z) \rangle = D^2(z) \int \frac{d^3 k}{(2\pi)^3} \frac{P_{\text{DM}}(k)}{(1 + x_b^2(z)k^2)^2}. \quad (8)$$

Hence,

$$A = n_0(z) e^{-\Delta^2(z)/2} \quad (9)$$

and

$$n_B(\mathbf{x}, z) = n_0(z) \exp[\delta_B(\mathbf{x}, z) - \frac{\Delta^2(z)}{2}]. \quad (10)$$

The lognormal distribution was introduced by Coles & Jones (1991) as a model for the non-linear matter distribution in the universe. When the density contrast is small ($\delta_B \ll 1$), equation (10) reduces to $n_B/n_0 \simeq 1 + \delta_B$, which is just what we expect from linear theory. On small scales, equation (10) becomes the isothermal hydrostatic solution, which describes highly clumped structures like intracluster gas, $n_B \propto \exp(-\mu m_p \psi_{\text{DM}}/\gamma k_B T)$, where ψ_{DM} is the dark matter potential (Sarazin & Bahcall 1977). The lognormal assumption has been used to model the IGM in numerical simulations (Bi 1993; Bi & Davidsen 1997) and is found to be working well in reproducing the observations. In particular, the simulation results matches well with the observed column density distribution and number density of the Ly α absorption lines, the probability distribution of the b parameter etc (see Bi & Davidsen 1997). [The analysis described below can, however, easily be carried out for any other local ansatz for the non-linear baryonic density. The results for power law assumption in which $n_B \propto (1 + \delta)^p$ will be discussed in a later paper.]

The fraction of hydrogen in the neutral form, f , in the IGM can be obtained by solving the ionisation equilibrium equation

$$\alpha(z, T(z)) n_p n_e = J(z) n_{\text{HI}}, \quad (11)$$

where $\alpha(z, T(z))$ is the radiative recombination rate and $J(z)$ is rate of photoionisation for hydrogen at redshift z

(Black 1981); n_p , n_e and n_{HI} are the number densities of proton, electron and neutral hydrogen, respectively. For simplicity, we assume that hydrogen is the only element present in the IGM and neglect the presence of helium and other heavier elements. In such a case, we have $n_e = n_p$. (This relation is not valid in the presence of helium or other heavier elements. If we have taken their presence into account, we would have got $n_e = \kappa n_p$, where κ is a constant. Usually, $1 \leq \kappa \leq 1.2$, because the amount of helium and heavier elements in the IGM is small compared to hydrogen. Since we do not know $J(z)$ beyond an accuracy of 10-20%, we can always absorb κ into $J(z)$.) Let us define the neutral fraction of hydrogen, f by

$$f = \frac{n_{\text{HI}}}{n} = \frac{n_{\text{HI}}}{n_{\text{HI}} + n_p} \quad (12)$$

Hence we get from equation (11)

$$\frac{(1 - f)^2}{f} = \frac{J(z)}{\alpha(z, T(z)) n_B}. \quad (13)$$

In general, one can solve this equation and determine f as a function of n_B . This expression simplifies for two extreme cases. For $f \ll 1$, we get

$$f = \frac{\alpha(z, T(z)) n_B}{J(z)} \quad (14)$$

and for $f \sim 1$,

$$f = 1 - \sqrt{\frac{J(z)}{\alpha(z, T(z)) n_B}}. \quad (15)$$

Hence, we have

$$n_{\text{HI}}(\mathbf{x}, z) = \begin{cases} \frac{\alpha(z, T(z))}{J(z)} n_B^2(\mathbf{x}, z) & (\text{if } n_{\text{HI}} \ll n_B) \\ n_B(\mathbf{x}, z) - \sqrt{\frac{J(z) n_B(\mathbf{x}, z)}{\alpha(z, T(z))}} & (\text{if } n_{\text{HI}} \sim n_B) \end{cases} \quad (16)$$

The ionisation conditions in the Ly α absorbers are similar to the of H II regions with $f \simeq 10^{-4}$. Thus, from now on we concentrate only on the case $n_{\text{HI}} \ll n_B$.

We take the temperature dependence of the recombination coefficient α to be given by (Rauch et al. 1997)

$$\alpha(z, T(z)) = \alpha_0(z) \left(\frac{T(z)}{10^4 K} \right)^{-0.7}, \quad (17)$$

where $\alpha_0 = 4.2 \times 10^{-13} \text{ cm}^3 \text{ s}^{-1}$. This relation is a good approximation for α in the temperature range relevant for Ly α forest. The temperature T is related to the baryonic density n through the equation of state. We assume a polytropic equation of state $p \propto \rho^\gamma \propto n^\gamma$, or equivalently

$$T(z) = T_0(z) [n_B(z)/n_0(z)]^{\gamma-1}, \quad (18)$$

where

$$n_0(z) = (\Omega_{\text{baryon}} h^2 \rho_c / m_p) (1 + z)^\beta \quad (19)$$

is the mean baryonic number density at redshift z . Then, the H I density becomes

$$n_{\text{HI}}(\mathbf{x}, z) = F(z) \left(\frac{n_B(\mathbf{x}, z)}{n_0(z)} \right)^\beta \quad (20)$$

where

$$F(z) = \alpha_0(z) n_0^2(z) \left(\frac{T_0(z)}{10^4 K} \right)^{-0.7} J^{-1}(z) \quad (21)$$

and

$$\beta = 2.7 - 0.7\gamma. \quad (22)$$

It is clear from equation (20) that we must have $\beta > 0$. But β can become negative if $\gamma > 3.86$. Usually for the IGM, γ lies in the range $1.2 < \gamma < 1.7$ (Schaye et al. 1999b). Hence, from now on, we need not worry about the sign of β . We can write the H I density in terms of the linear baryonic density contrast

$$n_{\text{HI}}(\mathbf{x}, z) = F_1(z) \exp[\beta \delta_B(\mathbf{x}, z)], \quad (23)$$

where

$$F_1(z) = F(z) e^{-\beta \Delta^2(z)/2}. \quad (24)$$

It is clear from equation (23) that the H I distribution at a particular redshift is also described by a lognormal distribution. All the statistical quantities regarding H I can be derived from this in a straightforward manner.

2.1 Correlation Function for Neutral Hydrogen

One of our main interest is the correlation function

$$\langle n_{\text{HI}}(\mathbf{x}, z) n_{\text{HI}}(\mathbf{x}', z') \rangle = F_1(z) F_1(z') \langle \exp\{\beta[\delta_B(\mathbf{x}, z) + \delta_B(\mathbf{x}', z')]\} \rangle, \quad (25)$$

from which several useful quantities can be obtained. Since δ_B is a Gaussian random field, we can write, using equation (7)

$$\langle \exp\{\beta[\delta_B(\mathbf{x}, z) + \delta_B(\mathbf{x}', z')]\} \rangle = \exp\left[\frac{\beta^2}{2}\{\Delta^2(z) + \Delta^2(z') + 2Q(\mathbf{x}, \mathbf{x}'; z, z')\}\right], \quad (26)$$

where

$$Q(\mathbf{x}, \mathbf{x}'; z, z') = \langle \delta_B(\mathbf{x}, z) \delta_B(\mathbf{x}', z') \rangle. \quad (27)$$

Simple algebra gives

$$Q(\mathbf{x}, \mathbf{x}'; z, z') \equiv Q(\mathbf{x} - \mathbf{x}'; z, z') = D(z) D(z') \int \frac{d^3 k}{(2\pi)^3} \frac{P_{\text{DM}}(k) e^{i\mathbf{k} \cdot (\mathbf{x} - \mathbf{x}')}}{(1 + x_b^2(z) k^2)(1 + x_b^2(z') k^2)}. \quad (28)$$

One also notes from equations (8) and (28) that $\Delta^2(z) = Q(0; z, z)$. We can now write equation (25) as

$$\langle n_{\text{HI}}(\mathbf{x}, z) n_{\text{HI}}(\mathbf{x}', z') \rangle = F_2(z) F_2(z') e^{\beta^2 Q(\mathbf{x} - \mathbf{x}'; z, z')}, \quad (29)$$

where

$$F_2(z) = F_1(z) e^{\beta^2 \Delta^2(z)/2}. \quad (30)$$

One needs to normalise the quantity $\langle n_{\text{HI}}(\mathbf{x}, z) n_{\text{HI}}(\mathbf{x}', z') \rangle$, to obtain the correlation function $\xi_{\text{HI}}(\mathbf{x} - \mathbf{x}'; z, z')$ for H I. A natural way of normalising the correlation would be to use the definition

$$1 + \xi_{\text{HI}}(\mathbf{x} - \mathbf{x}'; z, z') = \frac{\langle n_{\text{HI}}(\mathbf{x}, z) n_{\text{HI}}(\mathbf{x}', z') \rangle}{\langle n_{\text{HI}}(\mathbf{x}, z) \rangle \langle n_{\text{HI}}(\mathbf{x}', z') \rangle}. \quad (31)$$

Since $\langle n_{\text{HI}}(\mathbf{x}, z) \rangle = F_2(z)$, we get

$$\xi_{\text{HI}}(\mathbf{x} - \mathbf{x}'; z, z') = e^{\beta^2 Q(\mathbf{x} - \mathbf{x}'; z, z')} - 1 \quad (32)$$

with Q given by equation (28).

All the analysis above is valid if one can probe any scale with arbitrary accuracy. But it turns out that one cannot

obtain information about scales smaller than some particular value, due to various observational constraints. While observing along a LOS, it will be impossible to probe the velocity scales less than the spectroscopic limit due to thermal broadening and the blending of spectral lines. Similarly, while observing across the transverse direction, the peculiar velocities of individual points will constrain the velocity resolution which we have not taken into account in the above analysis. If Δv is the smallest scale one can probe, then the corresponding limit in the redshift-space is

$$\Delta z = \frac{\Delta v}{c}(1 + z). \quad (33)$$

This means that we will not be able to probe below a comoving length scale given by

$$\Delta x = d_H(z) \Delta z, \quad (34)$$

where

$$\begin{aligned} d_H(z) &= c \left(\frac{\dot{a}}{a} \right)^{-1} \\ &= \frac{c}{H_0} [\Omega_\Lambda + \Omega_m (1 + z)^3 + \Omega_k (1 + z)^2]^{-1/2}, \end{aligned} \quad (35)$$

$$\Omega_k = 1 - \Omega_m - \Omega_\Lambda. \quad (36)$$

This effect can be included in our calculation by smoothing over all the length scales smaller than Δx . We use a Gaussian window of width $\sigma_x = \Delta x$, and get a smoothed version of Q in equation (28). In Fourier space, this smoothing will introduce an extra Gaussian term in the integrand, and our smoothed Q will be

$$\begin{aligned} Q_{\text{smooth}}(\mathbf{x} - \mathbf{x}'; z, z') &= D(z) D(z') \int \frac{d^3 k}{(2\pi)^3} \frac{P_{\text{DM}}(k) e^{-k^2 \sigma_x^2/2} e^{i\mathbf{k} \cdot (\mathbf{x} - \mathbf{x}')}}{(1 + x_b^2(z) k^2)(1 + x_b^2(z') k^2)}. \end{aligned} \quad (37)$$

The angular integrations can be carried out trivially, and we get

$$\begin{aligned} Q_{\text{smooth}}(\mathbf{x} - \mathbf{x}'; z, z') &= \frac{D(z) D(z')}{2\pi^2} \int_0^\infty dk \frac{P_{\text{DM}}(k) k^2 e^{-k^2 \sigma_x^2/2}}{(1 + x_b^2(z) k^2)(1 + x_b^2(z') k^2)} \frac{\sin kX}{kX}, \end{aligned} \quad (38)$$

where $X = |\mathbf{x} - \mathbf{x}'|$. The final integration can be done numerically, once the DM power spectrum is given.

At this stage, the relations derived above can be used for any $\mathbf{x}, \mathbf{x}', z, z'$. As we mentioned earlier, if one observes the H I along a particular LOS, then one is probing different regions of the IGM at different redshifts. The position x will be related to the redshift z by the relation

$$x(z) = \int_0^z dH(z') dz' \quad (39)$$

where $dH(z)$ is given by equation (35). Then the LOS correlation function is given by

$$\xi_{\text{HI}}^{\text{LOS}}(z, z') = e^{\beta^2 Q_{\text{LOS}}(l(z, z'); z, z')} - 1, \quad (40)$$

where

$$\begin{aligned} Q_{\text{LOS}}(l(z, z'); z, z') &= \frac{D(z) D(z')}{2\pi^2} \int_0^\infty dk \frac{P_{\text{DM}}(k) k^2 e^{-k^2 \sigma_x^2/2}}{(1 + x_b^2(z) k^2)(1 + x_b^2(z') k^2)} \frac{\sin kl}{kl}, \end{aligned} \quad (41)$$

and

$$l(z, z') = x(z) - x(z'). \quad (42)$$

It should be stressed that $\xi_{\text{HI}}^{\text{LOS}}(z, z') \neq \xi_{\text{HI}}^{\text{LOS}}(z - z')$. This means that one cannot rigorously define a power spectrum from the LOS correlation function because the correlation is a function of *two* variables z and z' . *In other words, the LOS power spectrum does not exist in strict sense.* However, one can get an approximate LOS power spectrum for a small redshift range around any mean redshift. This can be done by defining an average redshift

$$\bar{z} = \frac{1}{2}(z + z'), \quad (43)$$

a redshift difference

$$\Delta z = z - z' \quad (44)$$

and evaluating the correlation function for a particular value of \bar{z} as a function of Δz . For small Δz , one can use equation (34) to write the correlation as a function of Δx and Fourier transform the correlation, and get the power spectrum. Such a power spectrum will depend on the value of \bar{z} . We stress again this power spectrum is approximate in the sense that it exists only for $\Delta z \ll \bar{z}$.

The transverse correlation is observed at some particular redshift ($z = z'$), along the transverse direction. Then

$$\xi_{\text{HI}}^{\text{trans}}(l_{\perp}; z) = e^{\beta^2 Q_{\text{trans}}(l_{\perp}; z)} - 1, \quad (45)$$

$$\begin{aligned} Q_{\text{trans}}(l_{\perp}; z) = & \\ & \frac{D^2(z)}{2\pi^2} \int_0^\infty dk \frac{P_{\text{DM}}(k) k^2 e^{-k^2 \sigma_x^2/2}}{(1 + x_b^2(z) k^2)^2} \frac{\sin kl_{\perp}}{kl_{\perp}}, \end{aligned} \quad (46)$$

where l_{\perp} is the comoving distance along the transverse direction. For a given redshift, the transverse correlation is only a function of l_{\perp} . Hence, one can obtain the power spectrum from $\xi_{\text{HI}}^{\text{trans}}$ following usual methods.

2.2 Column Density Distribution

One of the other statistics the observers use to quantify the distribution Ly α absorption lines is column density distribution. Indeed one can get the analytic expression for this using the formalism developed so far in this work. Note that Voigt profile fitting to the absorption lines are used to get the observed column density distribution. Here we use a method called ‘density-peak ansatz’ (DPA), discussed in Gnedin & Hui (1996) and Hui, Gnedin & Zhang (1997) to derive an analytic expression for the column density distribution.

Suppose we are looking at the IGM along any one direction, at some redshift z . Then the linear density field $\delta_B^{(1D)}(x, z)$ along that LOS will be described by a one dimensional Gaussian random field. DPA assumes that each density peak in the comoving space is associated with an absorption line, and one can assign a definite column density to each of them. In the articles referred above, each density peak is fitted with a Gaussian, and the column density is calculated using

$$N_{\text{HI}} \propto \int_{\text{peak}} n_{\text{HI}}(x) dx. \quad (47)$$

In such a case, there is a definite correlation between the value of the density field at the peak, and the effective width of the absorber (which is determined by the correlation between the density field and its second derivative at the peak, and is fixed once the fitting function for the density peak is given). We, however, take a simpler approach in assigning the column density to a density peak, which is described below.

The coherence scale of the distribution is defined as (Bardeen et al. 1986)

$$R^* \equiv \frac{\sigma_1}{\sigma_2}, \quad (48)$$

where σ_1 and σ_2 are defined in equation (A3) (see Appendix A). This length is a measure of the distance between two successive zeroes for the one dimensional Gaussian random field. Since this is the relevant scale for the distribution of zero-crossing, we expect the effective length scale of a peak to be a fraction of R^* . Then the column density corresponding to a particular peak will be

$$N_{\text{HI}} \propto n_{\text{HI}}[\text{peak}] R^* = n_{\text{HI}}[\text{peak}] R^* \epsilon \quad (49)$$

where $n_{\text{HI}}[\text{peak}]$ is the H I number density at the peak and ϵ is the proportionality constant, which can be used as a free parameter in comparing with observations. We have assumed ϵ to be independent of N_{HI} , which means that the column density is directly proportional to the peak density. Using this prescription for obtaining the column density from the H I density, we can easily obtain the relation between N_{HI} and $\delta_B^{(1D)}$, using equations (16) and (10). For the case $n_{\text{HI}} \ll n_B$, the relation is given by

$$\delta_B^{(1D)}[\text{peak}] = \frac{1}{\beta} \ln \left(\frac{N_{\text{HI}}}{R^* \epsilon F(z)} \right) + \frac{\Delta^2}{2} \quad (50)$$

Given this relation, it is straightforward to obtain the column density distribution $dN_{\text{pk}}/(dz dN_{\text{HI}})$. For completeness, we give the relevant calculations in the appendix.

3 RESULTS

3.1 LOS Correlation

We shall now compute the results for the H I correlation function for different scenarios. The parameters defining the model can be divided into two categories : (i) cosmological parameters, and (ii) parameters related to the IGM.

The first set of the cosmological parameters are those which determine the background cosmology. We assume that the background universe is described by the FRW metric. We have considered three different cosmological models. The model parameters are listed below:

SCDM $\Omega_m = 1, \Omega_\Lambda = 0, h = 0.5$

OCDM $\Omega_m = 0.35, \Omega_\Lambda = 0, h = 0.5$

LCDM $\Omega_m = 0.35, \Omega_\Lambda = 0.65, h = 0.5$

The next cosmological input that is required is the form of the DM power spectrum. We take the following form for $P_{\text{DM}}(k)$ (Efstathiou, Bond & White 1992)

$$P_{\text{DM}}(k) = \frac{Ak}{(1 + [ak + (bk)^{1.5} + (ck)^2]^\nu)^{2/\nu}} \quad (51)$$

where $\nu = 1.13$, $a = (6.4/\Gamma)h^{-1}$ Mpc, $b = (3.0/\Gamma)h^{-1}$ Mpc, $c = (1.7/\Gamma)h^{-1}$ Mpc and $\Gamma = \Omega_m h$. The normalisation parameter A is fixed through the value of σ_8 (the rms density fluctuation in spheres of radius $8 h^{-1}$ Mpc). We take the values of σ_8 to be given by (Eke, Cole & Frenk 1996)

$$\sigma_8 = \begin{cases} (0.52 \pm 0.04)\Omega_m^{-0.46+0.10\Omega_m} & (\text{if } \Omega_\Lambda = 0) \\ (0.52 \pm 0.04)\Omega_m^{-0.52+0.13\Omega_m} & (\text{if } \Omega_\Lambda = 1 - \Omega_m) \end{cases} \quad (52)$$

The next set of parameters are related to the IGM. We will model the IGM with two parameters: (i) the slope of the equation of state (γ) and (ii) the density averaged temperature (T_m). (We have already assumed that the equation of state for the IGM is polytropic $p \propto \rho^\gamma$.) It is known that the value of γ , at any given epoch, depends on the reionisation history of the universe (Hui & Gnedin 1999). The value of γ and its evolution is still pretty uncertain. Using Voigt profile fits to the observed Ly α absorption lines one can in principle obtain the value of γ . Available observations are consistent with γ in the range $1.2 < \gamma < 1.7$ (Schaye et al. 1999b) for $2 \leq z \leq 4.5$. The density averaged temperature is defined as,

$$T_m = \frac{\int \rho(T) T dT}{\int \rho(T) dT} \quad (53)$$

Using the equation of state $T \sim \rho^{\gamma-1}$, we get

$$T_m = \frac{2\gamma - 1}{\gamma} (T_{\max} - T_{\min}). \quad (54)$$

We take T_m to be in the range $20,000 \text{ K} < T_m < 60,000 \text{ K}$. This corresponds to b parameter in the range $18.3 \text{ km s}^{-1} < b < 31.7 \text{ km s}^{-1}$ and is consistent with the minimum value of b observed at higher H I column densities (i.e. $10^{14.5} \text{ cm}^{-2}$).

As we have discussed earlier, we need to smooth the power spectrum below some velocity because the blending of spectral lines makes it impossible to resolve the lines below a particular velocity. Typically this velocity is of the order of a few tens km s $^{-1}$. For definiteness, we take the smoothing velocity to be $\Delta v = 30 \text{ km s}^{-1}$.

We can now calculate ξ_{LOS} for any value of z and z' . As discussed earlier, we shall calculate the correlation function is for a particular mean redshift \bar{z} and plot it as a function of redshift difference Δz . One can convert Δz into a velocity $v = c\Delta z/(1 + \bar{z})$ and can obtain ξ_{LOS} as a function of v .

The results for the LOS correlation function for different cosmological models are shown in Figure 1. We have chosen typical values for T_m as 40,000 K and $\gamma = 1.5$, at a redshift of $\bar{z} = 2.5$. It can be seen that the correlation curves tend to flatten at low velocities, and drops at high velocities. The correlation curve in the LCDM model falls less rapidly compared to other two models. It is clear that the introduction of a cosmological constant makes the correlation curve flatter (the LCDM curve is flatter than the OCDM curve), and the curve is more or less independent of the matter density (compare the OCDM and SCDM curves). Since we have normalised the correlation with respect to zero separation scale, we cannot compare the absolute values directly, only the shapes can be compared.

We would like to compare our results with observational data. For this, we obtain the observational data from Cristiani et al. (1997). The data consists of several QSO spectra at various redshifts, ranging from 1.7 to 3.7. This range is

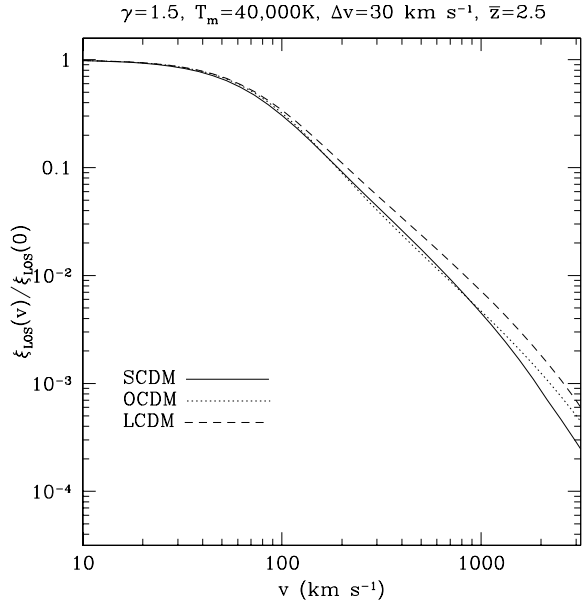


Figure 1. LOS correlation function as a function of velocity. Results for three different cosmological models at a mean redshift of $\bar{z} = 2.5$ are presented. The correlation function is normalised in such a way that it is unity at zero velocity separation.

pretty large, and evolutionary effects will be significant in the data. We compare the observed LOS correlation (points with error bars) with the theoretical curve for the three cosmological models, and for various ranges of values of T_m and γ in Figure 2 for $\bar{z} = 2.5$.

It is clear (see Figure 2) that increasing the density averaged temperature, T_m , or the slope of the equation of state, γ , make the correlation curves flatter. The changes in the correlation due to these two parameters are roughly of the same order. For example, the correlation curve with $T_m = 60,000 \text{ K}$, $\gamma = 1.2$ is nearly similar to the curve with $T_m = 20,000 \text{ K}$, $\gamma = 1.7$, for all the models. It seems that higher values of T_m and γ are preferred by the observations. It is interesting to note that the IGM parameters have stronger influence, compared to the cosmological parameters, on the shape of the correlation curves. This means we can constrain the IGM parameters by studying the velocity dependence of LOS correlation function even with ill-constrained cosmological parameters. However, it is not possible to constrain both T_m and γ simultaneously because the variation due to these two parameters are roughly the same. We would like to point here that the observational data points were obtained using the Ly α clouds with $\log(N_{\text{HI}}/\text{cm}^2) > 14$. However we have not used any such constraint while obtaining the analytical curves. As a preliminary check, we can see that the analytical curves have the broad features which are expected from the observational data. However, no quantitative statement can be made unless the observed LOS correlation is obtained using an extended dataset over a narrow range of redshift so that the evolutionary effects are minimised.

We next check the redshift evolution of the LOS correlation function. For definiteness, we consider ξ_{LOS} at a particular velocity, $v = 100 \text{ km s}^{-1}$, and plot it as a function of \bar{z} (Figure 3). The curves are normalised in such a

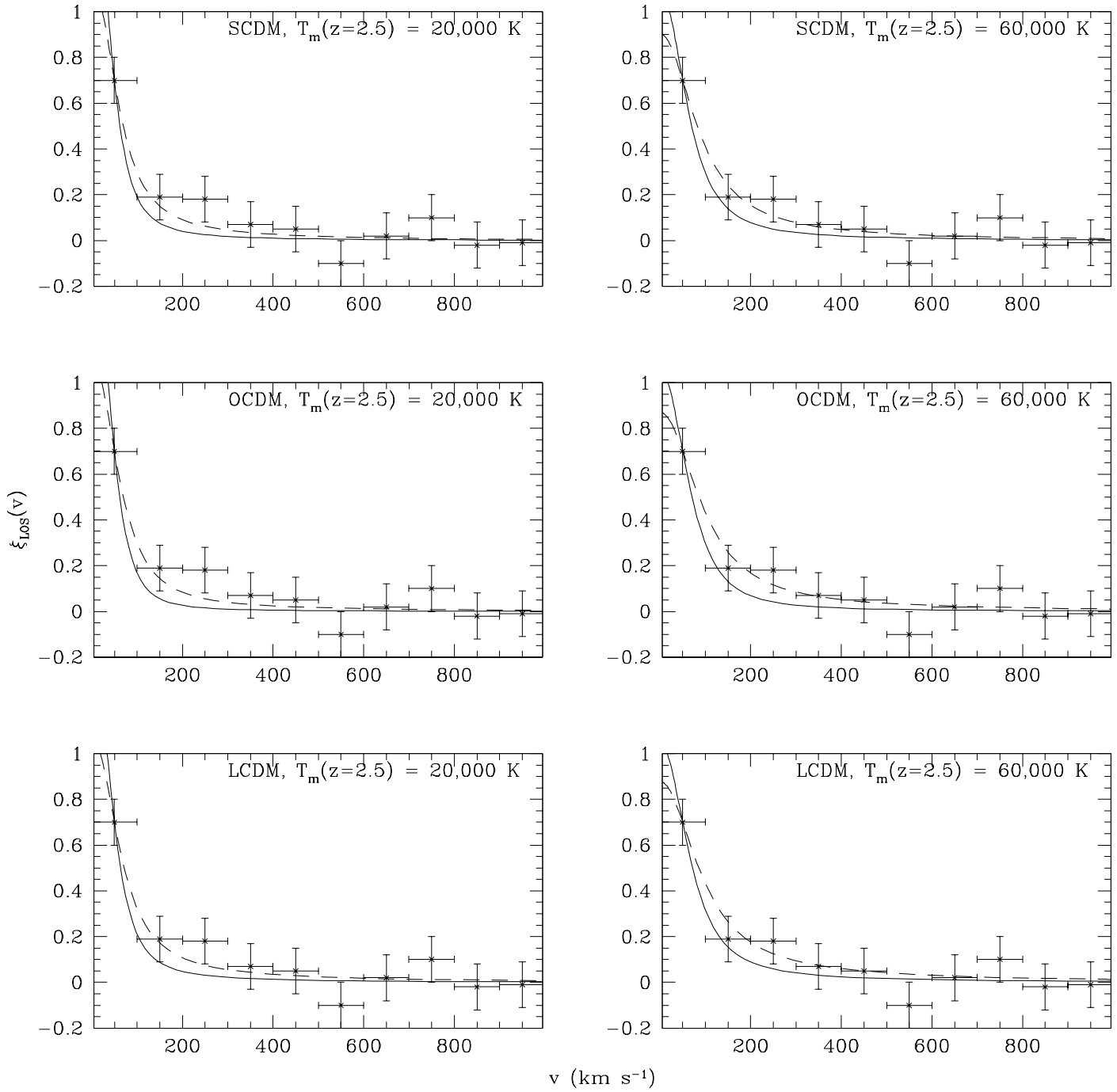


Figure 2. Comparison of the theoretical ξ_{LOS} with observational data (Cristiani et al. 1997). The solid and the dashed curves are for $\gamma = 1.2$ and $\gamma = 1.7$ respectively. The theoretical curves have been normalised in such a way that they match with the observed data point at the lowest velocity bin.

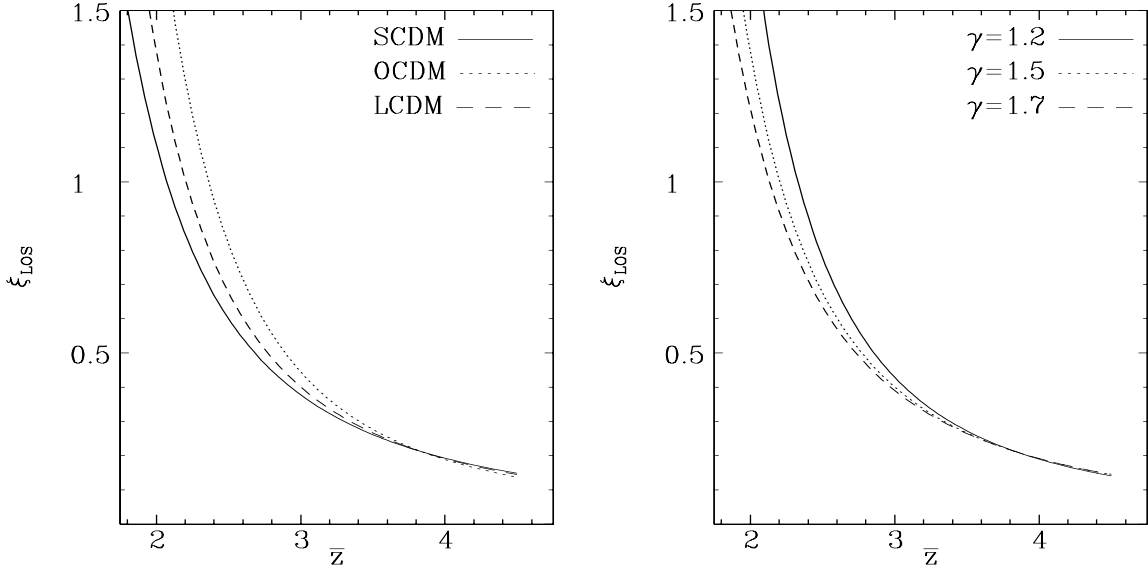


Figure 3. $\xi_{\text{LOS}}(v=100 \text{ km s}^{-1})$ as a function of \bar{z} . The curves are normalised in such a way that $\xi_{\text{LOS}}(v=100 \text{ km s}^{-1}) = 0.21$ at $\bar{z} = 3.85$, which is taken from Cristiani et al.(1997). In the left plot, the IGM parameters are fixed $T_m = 40,000 \text{ K}$, $\gamma = 1.5$. In the right plot, we have fixed the cosmological model to be LCDM, and $T_m = 40,000 \text{ K}$.

way that $\xi_{\text{LOS}}(v=100 \text{ km s}^{-1}) = 0.21$ at $\bar{z} = 3.85$, which is taken from Cristiani et al.(1997). We have assumed that γ does not evolve with redshift. The value of T_m is fixed at a particular redshift (in this case, at $\bar{z} = 2.5$) and the value of T_m at other redshifts are calculated using the relation $T_m \sim \rho^{\gamma-1} \sim (1+z)^{3\gamma-3}$.

We found the dependence of evolution of ξ_{LOS} on T_m is negligible. Thus in what follows we concentrate on the effect of γ and the cosmological models. It is clear that the amplitude of the correlation function increases with time with the evolution being most rapid in OCDM and least in SCDM. Also, the evolution becomes more rapid as we decrease γ . *However, the effects due to change in cosmology and γ are of the same order, which means that we cannot constrain both the parameters simultaneously.* Thus the above analysis clearly suggest that it will be very difficult to recover the power spectrum of density fluctuations uniquely from the Ly α absorption lines without knowing the IGM parameters. However, the cosmological parameters determined through studies such as CMBR (and other data), can be used to constrain the equation of state (using the plot in the right in Figure 3). The important thing to note is that we can constrain γ with ill-constrained values of T_m .

Throughout this paper we have treated γ to be independent of z . However, there are indications that γ could change with z . Schaye et al. (1999a) notice that the temperature of the IGM has a sharp increase at $z = 3$ and decreases with decreasing redshift afterwards. They also notice that the slope of the equation of state become close to one at $z \simeq 3$ then increases with decreasing redshift. Theoretical calculations

suggest that γ increases with time and the rate of evolution depends on the reionisation epoch (Hui & Gnedin 1997). From Figure 3 we can infer that when γ becomes larger the rate of growth of ξ_{LOS} at a given velocity decreases. *Thus our study clearly suggests that the evolution of ξ_{LOS} at a given velocity can be used as probe of a reionisation and thermal history of the IGM once the cosmological model is fixed.*

3.2 Transverse Correlation

In this section we present the results for the transverse correlation. As before, we consider the same CDM power spectrum, and essentially the same range of the IGM parameters. The smoothing velocity is taken to be 30 km s^{-1} , which is the typical peculiar velocity of a blob in the IGM.

Given z , we calculate ξ_{trans} as a function of the transverse comoving distance l_{\perp} . One can then convert this length scale to an angular scale θ through the following relations.

$$\theta = \frac{l_{\perp}}{d_a^{\text{com}}(z)} \quad (55)$$

$$d_a^{\text{com}}(z) = \frac{c}{H_0 \sqrt{|\Omega_k|}} S_k \left(x(z) \frac{H_0}{c} \sqrt{|\Omega_k|} \right) \quad (56)$$

where Ω_k is given by equation (36), $x(z)$ is given by equation (39) and

$$S_k(r) = \begin{cases} \sin r & (\text{if } \Omega_k < 0) \\ r & (\text{if } \Omega_k = 0) \\ \sinh r & (\text{if } \Omega_k > 0) \end{cases} \quad (57)$$

Instead of plotting the correlation function directly, we plot the quantity $\mathcal{P}_\theta(\theta)$, which is defined as follows. The excess probability, over random background, of finding two neutral hydrogen overdense separated by a comoving transverse distance l_\perp is

$$\mathcal{P}_{l_\perp}(l_\perp)dl_\perp = \frac{\xi_{\text{trans}}(l_\perp; z)2\pi l_\perp dl_\perp}{4\pi[d_a^{\text{com}}(z)]^2}. \quad (58)$$

Using equation (55) we get the excess probability over random background of finding two neutral hydrogen overdense separated by an angle θ as

$$\begin{aligned} \mathcal{P}_\theta(\theta) d\theta &= \mathcal{P}_{l_\perp}(l_\perp) \frac{dl_\perp}{d\theta} d\theta \\ &= \frac{1}{2} \xi_{\text{trans}}(\theta) \theta d\theta. \end{aligned} \quad (59)$$

From Figure 4 it is clear that even the maximum excess probability of finding two H I overdense regions over an angular scale greater than few arc seconds is less than 1%. Observationally the distribution of H I along the transverse direction is probed by studying the common absorbers along the LOS towards closely spaced QSOs. The angular scales probed varies between few arc seconds and few arc minutes (Shaver et al. 1982; Shaver & Robertson 1983; Smette et al. 1992; Dinshaw et al. 1994; Bechtold et al. 1994; Croots et al. 1994; Bechtold & Yee 1994; Smette et al. 1995; D'Odorico et al. 1997; Petitjean et al. 1998). Based on our analysis it is most likely that the common absorbers seen in the spectra of closely spaced QSOs are most likely probe the transverse extent of the same overdense region rather than the clustering length scale of separate regions.

3.3 Difference between ξ_{trans} and ξ_{LOS}

It should be noted that for a given mean redshift, the values of the LOS and the transverse correlation functions need not be the same. This is because, when we observe along one LOS, we actually sample different points at different redshifts. In contrast to this, the transverse correlation is calculated at the same redshift. The effect of evolution in the LOS correlation makes it different from the transverse correlation.

To illustrate this point more clearly, let us first assume that x_b does not evolve with z (this corresponds to the equation of state where $\gamma = 4/3$). Then from equations (41) and (46), we see that for a given length scale l , the integrands in the two equations are identical. Hence, we get

$$\frac{Q_{\text{LOS}}}{Q_{\text{trans}}} = \frac{D(\bar{z} + \Delta z/2)D(\bar{z} - \Delta z/2)}{D^2(\bar{z})}, \quad (60)$$

where \bar{z} and Δz are defined in equations (43) and (44) respectively. The difference in the two correlation functions is now entirely due to the evolution of the power spectrum. Thus the two correlation functions will be nearly equal for small Δz but will start differing from each other for large Δz . In the general case when x_b evolves with z , the difference will be much more prominent.

This is indeed true, as one can see from Figure 5. For scales below $200 h^{-1}$ Mpc, the two correlation functions are nearly the same. But above such scales the two functions start differing appreciably. For the observations made in the scales of $10-100 h^{-1}$ Mpc, our analytical calculation shows

that one should not see any appreciable difference between LOS and transverse correlations. This can be used as an important tool determining the power spectrum (provided, of course, we know the IGM parameters and the correlation function completely). As we have argued earlier, one cannot get the power spectrum from the LOS correlation. But the power spectrum can be obtained from the transverse correlation in usual manner. Since the two correlations are identical for scales upto $100 h^{-1}$ Mpc, one can start from the LOS correlation, replace it with the transverse correlation, and obtain the power spectrum. Hence, below scales of $100 h^{-1}$ Mpc, the Fourier transform of ξ_{LOS} will give the power spectrum, but one should interpret this result in a proper manner.

3.4 Column Density Distribution

Unlike the correlation functions discussed above, the column density distribution dependents on $J(z), \Omega_{\text{baryon}}$ and $T_0(z)$ through $F(z)$ in equation (50). However, one can see from the definition of $F(z)$ (equations (21) and (19)) that the parameters $J(z), \Omega_{\text{baryon}}$ and $T_0(z)$ appear as a combination $\Omega_{\text{baryon}} h^2 J^{-1}(z) T_0^{-0.7}(z)$. Instead of considering the values of the above parameters separately, we fix the value of $F(z)$ to be $F(z) = 4.78 \times 10^{-11} \text{ cm}^{-3}$ (which corresponds to typical values like $\Omega_{\text{baryon}} h^2 = 0.02, J = 0.46 \times 10^{-12} \text{ s}^{-1}, T_0 = 10,000 \text{ K}$). We shall check the dependence of the column density distribution on the following parameters : (i) cosmological models, (ii) ϵ and (iii) γ . (We have checked and found the dependence of column density distribution on T_m to be very weak.)

In what follows we try to get constraints on our model parameters using the observed column density distribution obtained from Hu et al. (1995) and Kim et al. (1997) at three mean redshifts 2.31, 2.85 and 3.35. In Figure 6 we plot, the quantity $f(N_{\text{HI}})$, that is related to the quantity $(dN_{\text{pk}}/dz dN_{\text{HI}})$ through the relation (Bi & Davidsen, 1997)

$$f(N_{\text{HI}}) = (dN_{\text{pk}}/dz dN_{\text{HI}})/(1+z). \quad (61)$$

The observational data points are the points with errorbars in the figure.

In the left most panel of each row in Figure 6 we plot the predicted column density distribution for various cosmological models for a given set of IGM parameters ($\gamma = 1.2$ and $T_m = 20,000$) and $\epsilon = 0.1$. In all the redshift bins it is clear that the SCDM curves fall steeply at the higher column density end compared to other models. This is consistent with the results noted by Gnedin & Hui (1996). However, in our method of obtaining $f(N_{\text{HI}})$, the SCDM model can be made to fit the data by slightly increasing the value of ϵ . The OCDM and LCDM curves fit the observed distribution upto $\log N_{\text{HI}} \geq 14.0$ for $\epsilon = 0.1$. In the middle panel of each row in Figure 6 we plot the predicted distribution for the two assumed values of ϵ for LCDM with $\gamma = 1.2$ and $T_m = 20,000 \text{ K}$. It is clear that the observed distribution is consistent with $\epsilon = 0.1$. This means that, in the case of LCDM, the effective length of the overdense region is about $(1/10)$ of the coherence scale R^* . The value of R^* depends on the baryonic power spectrum, its typical value is of the order of few hundreds of Kpc; for LCDM model with $\gamma = 1.2, T_m = 20,000 \text{ K}$, we get $R^* = 360 h^{-1} \text{ Kpc}$. This

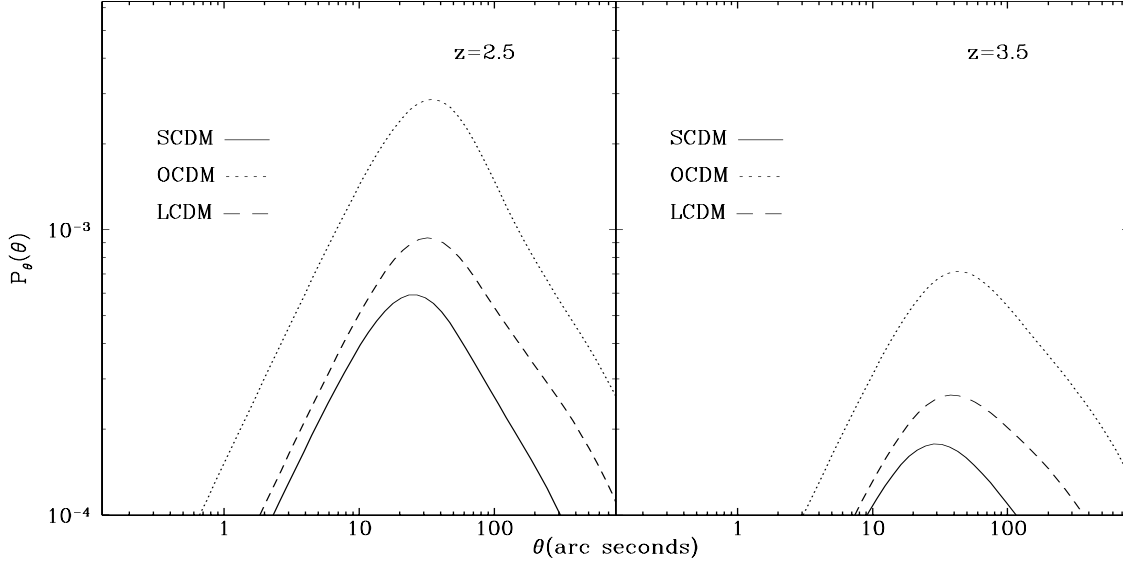


Figure 4. Plot of $\mathcal{P}_\theta(\theta)$. Results for three different cosmological models and for two different redshifts are presented. The IGM parameters are $\gamma = 1.5$, $T_m(z = 2.5) = 40,000\text{K}$. T_m at redshift $z = 3.5$ is calculated using the relation $T_m \sim (1 + z)^{3\gamma - 3}$.

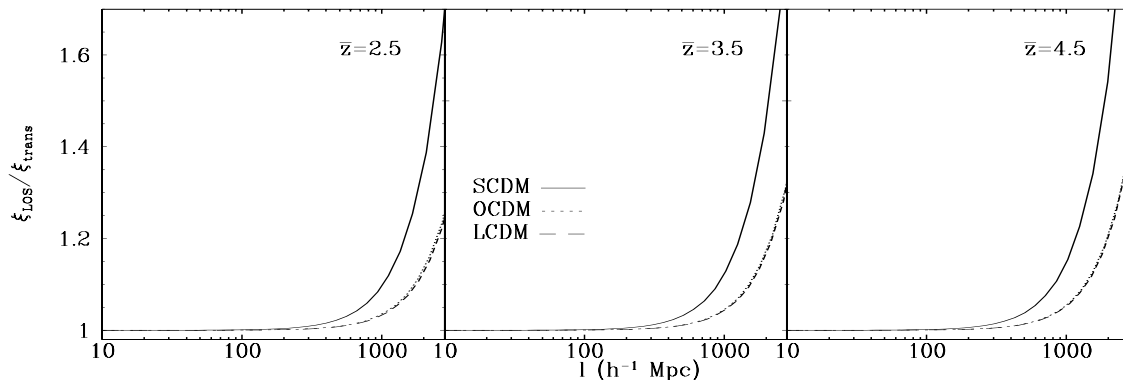


Figure 5. The ratio of ξ_{LOS} and ξ_{trans} as a function of comoving scale l . The results for three cosmological models and for three different mean redshifts are plotted. The curves for the LCDM and OCDM models nearly overlap.

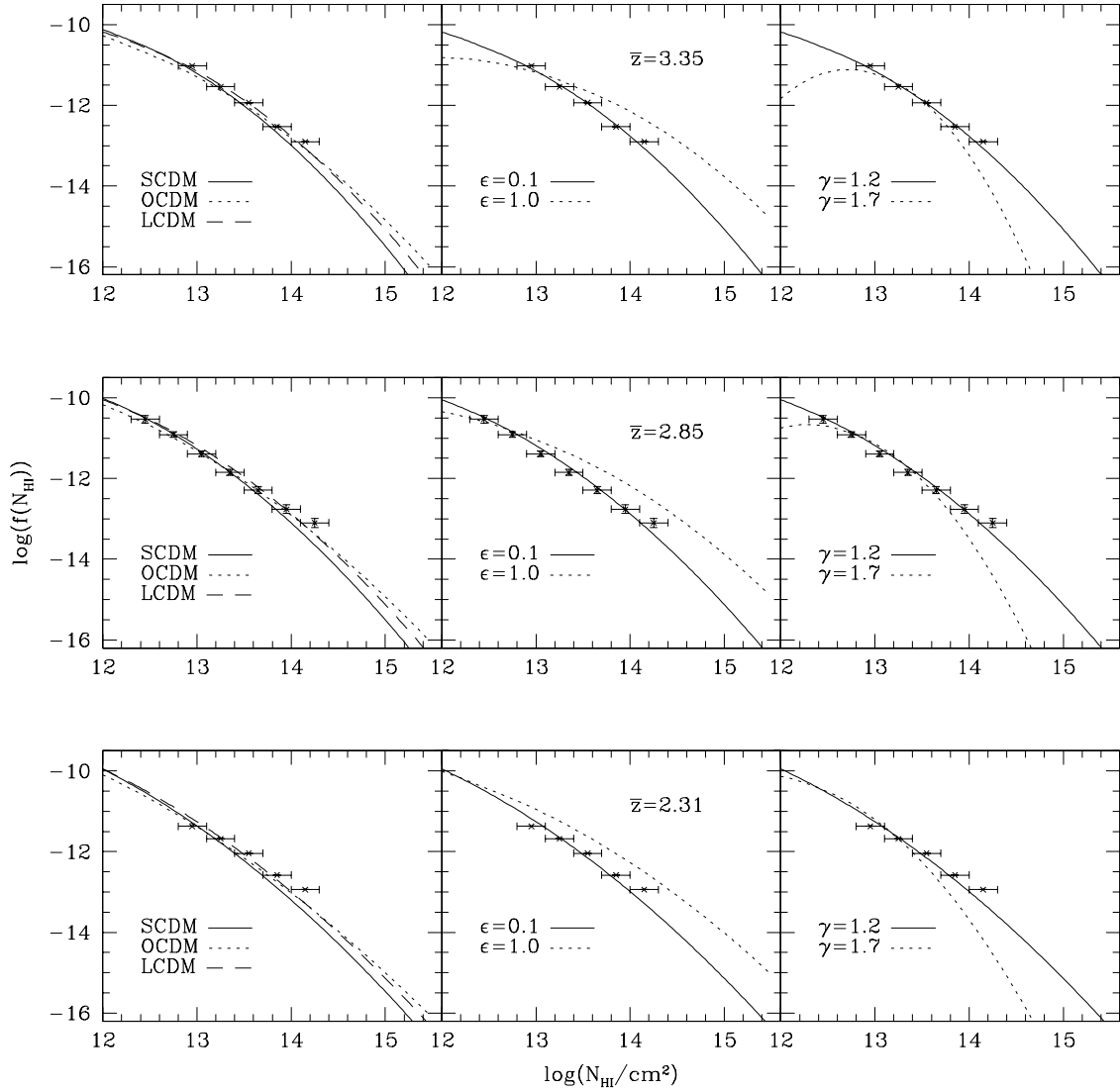


Figure 6. $f(N_{\text{HI}})$ as a function of N_{HI} for three redshifts. We show the dependence of $f(N_{\text{HI}})$ on cosmology (left), ϵ (center) and equation of state γ (right). For the left plots, we fix $\gamma = 1.2$, $T_m = 20,000\text{K}$, $\epsilon = 0.1$. The center plots are for the LCDM model with $\gamma = 1.2$, $T_m = 20,000\text{K}$. The right plots are also for LCDM with $T_m = 20,000\text{K}$, $\epsilon = 0.1$.

means that the typical length of an individual overdense region is $\sim 36h^{-1}\text{Kpc}$.

The effect of γ on the column density distribution can be seen from the right most panel in Figure 6 where we plot the results of LCDM model for two extreme values of γ . In the models with higher value of γ the $f(N_{\text{HI}})$ curve falls sharply at higher column density and at all redshifts. Also one can see the curve flattening in the low column densities. The effect seems to be more at the higher redshifts. It is clear, because of the flattening at the low column densities,

that lower values of γ are preferred for $\epsilon = 0.1$. However, one can get the consistent fit for higher values of γ by increasing the value of ϵ . At $\bar{z} = 2.31$, one can fit the data reasonably well with ϵ in the range 0.1 to 0.2 and γ in the range 1.2 to 1.6. For $\bar{z} = 2.85$ the corresponding ranges are $0.1 \leq \epsilon \leq 0.2$ and $1.2 \leq \gamma \leq 1.55$ and those for $\bar{z} = 3.35$ are $0.1 \leq \epsilon \leq 0.15$ and $1.2 \leq \gamma \leq 1.55$. It is impossible to fit the data with $\gamma > 1.6$, for any choice of ϵ at any redshift bin. As we noted before, the observed LOS correlation function, though affected by the evolutionary effects, at similar red-

shifts favours higher value of γ . One can get consistent fit to both the observations by increasing γ and ϵ as a function of redshift as predicted by standard reionisation models.

4 CONCLUSIONS

We have presented a simple analytic expression for the correlation function and the column density distribution for the low H I column density systems seen in the spectra of high redshift QSOs. We have used our results to get constraints on various cosmological and IGM parameters. We summarise our main results below.

1. One cannot rigorously define a power spectrum from the LOS correlation function. However, since the LOS and transverse correlations are identical below scales of $\sim 100 h^{-1}$ Mpc, it is possible to obtain the power spectrum by a Fourier transform of the LOS correlation function (provided the IGM parameters are known).

Previous studies have attempted to recover the power spectrum of density fluctuations from the observations of the IGM (Croft et al. 1998, Hui 1998, Croft et al. 1999). We show that it is difficult to recover a unique power spectrum from H I correlation function without constraining the IGM parameters, especially γ . We feel that the correct approach in studying this issue is to constrain the cosmological models using CMBR or supernovae data, and apply those constraints to study the IGM parameters using H I correlation functions.

2. The evolution of the LOS correlation function at a particular velocity depends on γ . For a given cosmological model, it is possible to constrain the value of γ at different epochs through these curves which, in turn, will constrain the evolution of γ . However, for such an exercise one needs accurate observational data at different redshift bins which are not affected by evolutionary effects. These constraints can also be used as an independent method to constrain the reionisation history of the universe.

3. The analytic column density distribution for H I, when compared with observations, favours a lower value of γ . We show that γ should be less than 1.6 for redshifts around 2.5 and should be less than 1.55 for redshifts 3 to 4. Also, the LOS correlation function and the column density distribution can be used simultaneously to put stringent constraints on γ and its evolution.

ACKNOWLEDGMENT

We gratefully acknowledge the support from the Indo-French Centre for Promotion of Advanced Research under contract No. 1710-1. TRC is supported by the University Grants Commission, India.

REFERENCES

Bardeen J. M., Bond J. R., Kaiser N., Szalay A. S., 1986, ApJ 304, 15
 Bechtold J., Crots A. P. S., Duncan R. C., Fang Y., 1994, ApJ 437, L83
 Bechtold J., Yee H. K. C., 1994, AJ 110, 1984
 Bergeron J., Boisse P., 1991, A&A 243, 344
 Bi H., 1993, ApJ 405, 479
 Bi H. G., Börner G., Chu Y., 1992, A&A 266, 1
 Bi H., Davidsen A. F., 1997, ApJ 479, 523
 Bi H., Ge J., Fang L., 1995, ApJ 452, 90
 Black J. H., 1981, MNRAS 197, 553
 Bond J. R., Szalay A. S., Silk J., 1988, ApJ 324, 627
 Cen R. Y., Miralda-Escudé J., Ostriker J. P., Rauch M. R., 1994, ApJ 437, L9
 Coles P., Jones B., 1991, MNRAS 248, 1
 Cristiani S., D'Odorico S., D'Odorico V., Fontana A., Giallongo E., Moscardini L., Savaglio S., 1997, in Petitjean P., Charlot S. eds., Proc. of the 13th IAP Astrophysics Colloquium, *Structure and Evolution of the Intergalactic Medium from QSO Absorption Line Systems*. Editions Frontières, Paris, p. 165
 Cristiani S., D'Odorico S., Fontana A., Giallongo E., Savaglio S., 1995, MNRAS 273, 1016
 Croft R. A. C., Weinberg D. H., Katz N., Hernquist L., 1998, ApJ 495, 44
 Croft R. A. C., Weinberg D. H., Pettini M., Hernquist L., Katz N., 1999, ApJ 520, 1
 Crots A. P. S., Bechtold J., Fang Y., Duncan R. C., 1994, ApJ 437, 79
 Davé R., Hernquist L., Katz N., Weinberg D. H., 1999, ApJ 511, 521
 Dinshaw N., Impey C. D., Foltz C. B., Weymann R. J., Chaffee F. H. Jr., 1994, ApJ 437, L87
 D'Odorico S., Cristiani S., D'Odorico V., Fontana A., Giallongo E., Shaver P., 1997, in Petitjean P., Charlot S. eds., Proc. of the 13th IAP Astrophysics Colloquium, *Structure and Evolution of the Intergalactic Medium from QSO Absorption Line Systems*. Editions Frontières, Paris, p. 392
 Doroshkevich A. G., Shandarin S. F., 1977, MNRAS 179, 95
 Efstathiou G., Bond J. R., White S. D. M., 1992, MNRAS 258, 1P
 Eke V. R., Cole S., Frenk C. S., 1996, MNRAS 282, 263
 Fang L. Z., Bi H., Xiang S., Börner G., 1993, ApJ 413, 477
 Gnedin Y. G., Hui L., 1996, ApJ 472, L73
 Hernquist L., Katz N., Weinberg D. H., Miralda-Escudé J., 1996, ApJ 457, L51
 Hui L., 1999, ApJ 516, 519
 Hui L., Gnedin Y. G., 1997, MNRAS 292, 27
 Hui L., Gnedin Y. G., Zhang Y., 1997, ApJ 486, 599
 Khare P., Srianand R., York D. G., Green R., Welty D., Huang K., Bechtold J., 1997, MNRAS 285, 167
 Kim T., Hu E. M., Cowie L. L., Songaila A., 1997, AJ, 114, 1
 McDonald P., Miralda-Escudé J., Rauch M., Sargent W. L. W., Barlow T. A., Cen R., Ostriker J. P., preprint (astro-ph/9911196)
 McGill C., 1990, MNRAS 242, 544
 Miralda-Escudé J., Cen R., Ostriker J. P., Rauch M., 1996, ApJ 471, 582
 Petitjean P., Surdej J., Smette A., Shaver P., Mücket J., Remy M., 1998, A&A 334, L45
 Riediger R., Petitjean P., Mücket J. P., 1998, A&A 329, 30
 Sarazin C. L., Bahcall J. N., 1977, ApJS 34, 451
 Schaye J., Theuns T., Leonard A., Efstathiou G., 1999a, MNRAS 310, 57
 Schaye J., Theuns T., Rauch M., Efstathiou G., Sargent W. L. W., 1999b, preprint (astro-ph/9912432)
 Shaver P. A., Boksenberg A., Robertson J. G., 1982, ApJ 261, L7
 Shaver P. A., Robertson J. G., 1983, ApJ 268, L57
 Smette A., Robertson J. G., Shaver P. A., et al., 1995, A&AS 113, 199
 Smette A., Surdej J., Shaver P. A., et al., 1992, A&A 389, 39
 Srianand R., 1997, ApJ 478, 511
 Steidel C. C., 1993, in Shull J. M. & Thronson H. A., Proc. of the 3rd Teton Astronomy Conference, *The Environment and Evolution of Galaxies*. Dordrecht, Kluwer, p. 263

Theuns T., Leonard A., Efstathiou G., 1998, MNRAS 297, L49
 Theuns T., Leonard A., Efstathiou G., Pearce F. R., Thomas P. A., 1998, MNRAS 301, 478
 Zhang Y., Anninos P., Norman M. L., 1995, ApJ 453 L57

APPENDIX A: DETAILED CALCULATIONS FOR THE COLUMN DENSITY DISTRIBUTION

Suppose we are looking at the IGM along any one direction, at some redshift z . Then the linear density field $\delta_B^{(1D)}(x, z)$ along that axis will be described by a one dimensional Gaussian random field, with a power spectrum

$$P_B^{(1D)}(k, z) = \frac{1}{2\pi} D^2(z) \int_k^\infty dk' k' \frac{P_{\text{DM}}(k)}{(1 + x_b^2(z) k'^2)^2} \quad (\text{A1})$$

From now on we shall derive all the expressions at a particular redshift z , and we shall not write the explicit z -dependence on the quantities.

To define the column density, we associate each local maximum or peak in the linear density field to a Ly α cloud. The column density corresponding to such a cloud is given by equation (49). We have expressed $\delta_B^{(1D)}$ [peak] in terms of N_{HI} in equation (50).

Using the properties of a Gaussian random field, we can derive the joint probability distribution for the three Gaussian random fields $\delta_B^{(1D)}, \delta_B^{(1D)\prime\prime}, \delta_B^{(1D)\prime}$. The probability that the field and its second derivative have values $\delta_B^{(1D)}$ and $\delta_B^{(1D)\prime\prime}$, respectively at the peak $\delta_B^{(1D)\prime} = 0$ is

$$\mathcal{P}[\delta_B^{(1D)}, \delta_B^{(1D)\prime\prime}, \delta_B^{(1D)\prime} = 0] d\delta_B^{(1D)} d\delta_B^{(1D)\prime\prime} |\delta_B^{(1D)\prime\prime}| dx = \frac{1}{(2\pi)^{3/2} \sigma_1 \Sigma} \exp \left[\frac{1}{2\Sigma^2} (\sigma_2^2 \delta_B^{(1D)} + 2\sigma_1^2 \delta_B^{(1D)} \delta_B^{(1D)\prime\prime} + \sigma_0^2 \delta_B^{(1D)\prime\prime\prime}) \right] d\delta_B^{(1D)} d\delta_B^{(1D)\prime\prime} |\delta_B^{(1D)\prime\prime}| dx, \quad (\text{A2})$$

where

$$\sigma_m^2 \equiv \sigma_m^2(z) = \frac{1}{2\pi} \int_{-\infty}^\infty dk k^{2m} P_B^{(1D)}(k, z), \quad (\text{A3})$$

and

$$\Sigma^2 = \sigma_0^2 \sigma_2^2 - \sigma_1^4. \quad (\text{A4})$$

Note that $\sigma_0 = \Delta$, defined in equation (8).

For convenience, let us define some dimensionless quantities

$$\nu \equiv \frac{\delta_B^{(1D)}}{\sigma_0}, \lambda \equiv -\frac{\delta_B^{(1D)\prime\prime}}{\sigma_2}, \kappa \equiv \frac{\sigma_1^2}{\sigma_0 \sigma_2} \quad (\text{A5})$$

ν and λ measure the field and its second derivative, respectively; κ is a measure of the width of the power spectrum. One can use these quantities to obtain the number of peaks (clouds) per unit length

$$\frac{dN_{\text{pk}}}{dx} = \mathcal{P}[\delta_B^{(1D)}, \delta_B^{(1D)\prime\prime}, \delta_B^{(1D)\prime} = 0] d\delta_B^{(1D)} d\delta_B^{(1D)\prime\prime} |\delta_B^{(1D)\prime\prime}| \quad (\text{A6})$$

Using equation (34), one can convert the above expression to the number of clouds per unit redshift interval. After simplification, the relation becomes

$$\frac{dN_{\text{pk}}}{dz} = \frac{d_H(z)}{(2\pi)^{3/2} \sqrt{1 - \kappa^2} R^*} \times$$

$$\exp \left[-\frac{1}{2} \left\{ \frac{(\nu - \kappa\lambda)^2}{1 - \kappa^2} + \lambda^2 \right\} \right] \lambda d\lambda d\nu \quad (\text{A7})$$

The λ integration can be carried out to obtain

$$\begin{aligned} \frac{dN_{\text{pk}}}{dz d\nu} = & \frac{d_H(z)}{(2\pi)^{3/2}} \left[\sqrt{1 - \kappa^2} \exp \left(-\frac{\nu^2}{2(1 - \kappa^2)} \right) \right. \\ & + \kappa\nu \sqrt{2\pi} e^{-\nu^2/2} \\ & \left. - \sqrt{\frac{\pi}{2}} \kappa\nu \operatorname{erfc} \left(\frac{\kappa\nu}{\sqrt{2(1 - \kappa^2)}} \right) e^{-\nu^2/2} \right] \end{aligned} \quad (\text{A8})$$

We are interested in the quantity

$$\frac{dN_{\text{pk}}}{dz dN_{\text{HI}}} = \frac{dN_{\text{pk}}}{dz d\nu} \frac{d\nu}{dN_{\text{HI}}} \quad (\text{A9})$$

which is straightforward to obtain from equation (A8), provided we know ν as a function of N_{HI} . Equations (50) and (A5) give ν in terms of N_{HI} , and they can be used to calculate $d\nu/dN_{\text{HI}}$ (for $n_{\text{HI}} \ll n_B$)

$$\frac{d\nu}{dN_{\text{HI}}} = \frac{1}{\beta \Delta N_{\text{HI}}}. \quad (\text{A10})$$

Thus we get an analytic expression for the number of clouds per unit redshift interval per unit column density range ($dN_{\text{pk}}/dz dN_{\text{HI}}$) as a function of N_{HI} .